Computers and Electronics in Agriculture 212 (2023) 108081

Contents lists available at ScienceDirect

Computers and Electronics in Agriculture

journal homepage: www.elsevier.com/locate/compag

Original papers

ECG augmented pulse oximetry in Atlantic salmon (*Salmo salar*)—A pilot study☆

E. Svendsen [a,b,*], M. Føre [a], L.L. Randeberg [c], R.E. Olsen [d], B. Finstad [d], M. Remen [b], N. Bloecher [b], J.A. Alfredsen [a]

[a] Department of Engineering Cybernetics, Norwegian University of Science and Technology, O.S. Bragstads plass 2D, Trondheim, 7034, Norway
[b] SINTEF Ocean AS, Brattørkaia 17C, Trondheim, 7010, Norway
[c] Department of Electronic Systems, Norwegian University of Science and Technology, O.S. Bragstads plass 2B, Trondheim, 7034, Norway
[d] Department of Biology, Norwegian University of Science and Technology, Brattørkaia 17B, Trondheim, 7010, Norway

ARTICLE INFO

Keywords:
Pulse oximetry
Light scattering
Motion artifact
Electrocardiogram
Least mean square filtering

ABSTRACT

Understanding the tolerance limits of fish is crucial for developing aquaculture operations that ensure good animal welfare. However, there exist little data describing the physiological responses in farmed Atlantic salmon, much because the technological tools for taking such measurements have not existed. Recent advances in electronic implants have enabled concurrent measurement of electrocardiogram (ECG) and photoplethysmograms (PPG) in salmon that can be used for robust estimation of HR and oxygen saturation in arterial blood (i.e., SpO_2/pulse oximetry) if appropriate strategies for motion artifact and light scattering compensation can be realized. To enable pulse oximetry for farmed Atlantic salmon (and fish in general), two experiments have been conducted. In Experiment 1, PPGs were obtained from salmon induced to swim at two different water currents under normoxic conditions. By using two water currents, the resulting data provided a foundation for developing methods for motion artifact compensation. Data from this experiment were also used to calculate an average light scattering parameter using the modified Beer–Lambert law, under the assumption that SpO_2 was 100 % for individual fish. In Experiment 2, fish were placed in a swim tunnel and subjected to hypoxic conditions and corresponding changes in SpO_2 were estimated using the motion artifact and light scattering compensation approaches from Experiment 1.

Results show that the suggested compensation approaches gives SpO_2 estimates within the expected range (95 % to 100 %) under normoxic conditions. Under hypoxic conditions, changes in SpO_2 that coincide with experiment events were observed, demonstrating that PPGs can be used to quantify such changes. The results from this pilot study therefore extend the selection of physiological parameters feasible to measure using electronic implants for Atlantic salmon. In doing so, the scope for physiological measurements is extended such that an improved understanding of physiological responses and tolerances in Atlantic salmon farming can be acquired, and ultimately be used to improve animal welfare in fish production.

1. Introduction

Aquaculture has grown into an important global food-producing industry with Atlantic salmon (*Salmo salar*) being one of the most popular farmed species. In Norway, 1.5 million tonnes were produced for worldwide consumption in 2022 (FDIR, 2023). Salmon production involves a broad range of farming operations (e.g., crowding, pumping, de-lousing and net cleaning) which may have negative impacts on fish health and welfare. Lack of real-time, objective physiological inputs to animal welfare and production control routines is a persistent challenge in Atlantic salmon farming and is difficult to detect and quantify. Despite extensive use of different sensing technologies (Føre et al., 2017b), current farming practices result in a 17% mortality rate during the sea phase (Sommerset et al., 2023). A part of this may be attributed to limited access to, and knowledge of, the tolerances of the fish in different farming contexts. Research tools that may increase such knowledge are miniaturized, implantable electronic sensing systems commonly referred to as 'tags' that can be used to directly measure physiological and behavioral parameters (Thorstad et al., 2013). Typical behavioral parameters possible to measure using existing off-the-shelf tags include

☆ This work was funded by the Research Council of Norway (RCN) (Project Number 280864) and through in-kind contribution by SINTEF Ocean AS.
* Corresponding author at: Department of Engineering Cybernetics, Norwegian University of Science and Technology, O.S. Bragstads plass 2D, Trondheim, 7034, Norway.
E-mail addresses: eirik.svendsen@ntnu.no, eirik.svendsen@sintef.no (E. Svendsen).

https://doi.org/10.1016/j.compag.2023.108081
Received 24 March 2023; Received in revised form 10 July 2023; Accepted 17 July 2023
Available online 29 July 2023

activity and swimming depth (Føre et al., 2011), and, more recently, the position of individual fish (Baktoft et al., 2017; Hassan et al., 2019), while physiological parameters obtainable in full scale salmon farming are currently limited to heart rate (HR) (Brijs et al., 2018).

To expand the selection of physiological measurements for farmed Atlantic salmon, a novel implant has been developed which measures PPGs (Svendsen et al., 2021b), i.e., the pulsatile change in tissue light absorption. The PPGs can be used to make HR estimates more robust (Svendsen et al., 2021c) and in principle, estimate oxygen saturation in arterial blood (SpO_2). This technique is referred to as *pulse oximetry* (PO) (Aoyagi, 2003; Wypych, 2013; Mannheimer, 2007), and successful implementation of PO may increase insight into the fish's physiological response, and by extension, its tolerances. This may be of use in salmon farming where low dissolved oxygen events may occur with negative impacts on the fish (Oppedal et al., 2011; Remen et al., 2013, 2016; Jónsdóttir et al., 2019).

PO is based on the Beer–Lambert law (BLL) and the assumption that arteries expand during heart contraction (systole) and contract during heart relaxation (diastole) (Kyriacou and Allen, 2021). Due to the higher blood profusion, light absorption in tissues will increase during systole and conversely decrease during diastole creating a pulsatile 'AC' component in the PPG. However, motion introduces artifacts (Motion Artifacts, MA) distorting the PPG, thus affecting SpO_2 accuracy (Chan et al., 2013). Before attempting to estimate SpO_2 using PPGs, MA must be reduced.

MA reduction is a persistent challenge in PPG signal processing. Common approaches to detect and reduce MA in human PPGs include morphology analysis (Sukor et al., 2011), thresholding of statistical moments (Hanyu and Xiaohui, 2017) and various filtering approaches using synthetic or accelerometer based Refs. Zhang et al. (2014), Casson et al. (2016), Xiong et al. (2016) and Dubey et al. (2018). Based on such references, the PPG can be (re)constructed using variants of principal component analysis (e.g., singular spectrum analysis (SSA) Golyandina et al., 2018). Such methods commonly focus on estimating HR rather than SpO_2, potentially causing information crucial for determining SpO_2 (i.e., the PPG pulse amplitude) to be degraded or lost. Furthermore, several of these approaches assume that MAs are separable from the PPG in the time and/or frequency domain. This may be true for human PPGs during physical exertions such as running. In the case of Atlantic salmon, co-inspection of PPG and inertial motion unit (IMU) data from free swimming fish suggest that MAs are generally oscillatory in nature and also appear within a frequency range close to the HR of the fish, meaning that conventional methods of MA reduction may remove too much of the PPG information required for SpO_2 estimation. This implies the need for an alternative approach. Considering that the pulsatile components in PPG are linked with the HR of the fish, a potential approach could be to extract the components of the PPG signal that share frequency properties with the HR and use these to estimate SpO_2, as this would effectually remove all components arising due to other phenomena, including MAs.

Furthermore, the BLL precludes that light travels in a non-scattering homogeneous medium. This is not the case for biological tissues. Using BLL, thus, requires that such effects are compensated. In humans, this is achieved empirically using reference oximeters by obtaining a baseline for comparison when human volunteers breathe a desaturated gas mixture. To the best of our knowledge, no reference oximeter for fishes exists, thus, excluding reference based empirical mapping. An alternative approach is to use the modified BLL (MBLL) which includes a scattering compensation term. This term can be calculated if SpO_2 is known or can be reasonably assumed. In this study, initial steps towards realizing PO in Atlantic salmon, are taken by conducting two experiments to derive a viable MA compensation approach and identify an average scattering compensation parameter that give credible results when combined. The purpose of Experiment 1 was, thus, to obtain PPG data under normoxic conditions that could be used to identify an average scattering correction parameter and develop an MA reduction/filtering approach and verify that its application results in an SpO_2 estimate within the expected range (i.e., 95% to 100%), while the purpose of Experiment 2 was to apply the processing methods and average scattering correction parameter from Experiment 1 to evaluate if the PO implant responded to changes in SpO_2.

2. Materials and methods

2.1. Ethical statement

The experiments were approved by the Norwegian Food Safety Administration under animal experiment permits 27 675 (Experiment 1) and 24 907 (Experiment 2). Data were obtained from 13 fish in total. After the experiments, all fish were euthanized using methods compliant with Appendix C in the Norwegian research animal regulations (FOR-2015-06-18-761, 2015).

2.2. Experiment animals

Atlantic salmon were held in an indoor tank ($2 \times 2 \times 1.6$ m) with a flow through sea water supply (30 l per min, 8.2 °C average temperature during the experiment period) from a 70 m deep intake in the Trondheimsfjord. The fish were fed in abundance using 5 mm pellets (EWOS HP 500 50 A 500) using 24 h lighting to facilitate growth. The tank was equipped with a water circulation pump (EMAUX Super-Power) with a tangential outlet to provide a water current of ≈ 1 body length per s (BLs^{-1}) at the tank periphery. A Sterner Oxyguard oxygenation system ensured water oxygen saturation ≥90%.

2.3. Pulse oximetry tag

The PO tag (Svendsen et al., 2021b) used in both experiments included a biosensor module (MAX86150, Maxim Integrated) measuring PPG at two wavelengths, $\lambda_1 = 660$ nm and $\lambda_2 = 880$ nm. The biosensor module also measured ECG via electrodes embedded in the implant's encapsulation. An inertial motion unit (IMU) measuring acceleration and rotation in three dimensions was also part of the implant design and were logged concurrently with PPG and ECG for activity evaluations. The implant was cylindrical in shape and measured 13 mm in diameter, 47 mm in length and weighing 9.4 g (in air)/6 g (in water) making it suitable for use in fish ≥ 600 g.

2.4. Experiment 1

Experiment 1 was conducted in an indoor tank that was identical to the holding tank and used the same water supply. The tank was covered by a thin, white tarpaulin taut over a pyramidal framework to shield the experiment animals from visual disturbances. Water oxygen saturation was maintained at $90 \pm 0.62\%$ (10.7 ± 0.07 mg L^{-1}) by a Sterner Oxyguard oxygenation system through the experiment. A water circulation pump (EMAUX Super-Power) was used to control water current speed at the tank periphery.

The experiment took place over 2 days. On day 1 between 12:20 and 15:00, PO tags were surgically implanted into the peritoneal cavity of five Atlantic salmon (fork length 53.5 ± 1.3 cm, weight 2426 ± 55.7 g, Foulton's K-factor 1.6 ± 0.1) captured randomly from their holding tank using a knotless dip net. Surgery was identical to the procedure described in literature for a similar tag type (Svendsen et al., 2021a; Føre et al., 2021), with an additional step of suturing a colored bead to the anterior root of the dorsal fin for visual identification purposes. After surgery each fish was placed in a wake-up tank with circulating sea water. After regaining consciousness, the fish was transferred to the experiment tank for habituation/recovery for 18 h to 20 h at ≈ 15 cm/s current.

On day 2, data collection started automatically and simultaneously for all fish at 09:00. The PO tags were programmed to sample data at 200 Hz in 1 min sampling bursts spaced by 1 min of idle time (i.e., a 1:2 duty cycle), which, given the internal storage space in the tag, allowed an experiment duration of 66 min. The (peripheral) current for the first 30 min was $\approx$ 15 cm/s and thereafter increased to $\approx$ 40 cm/s for the remaining 36 min.

After data collection, the fish were extracted using a knotless dip net and euthanized by an anesthetic overdose (Benzoak vet, 70 mg/L until level 4 anesthesia Coyle et al., 2004 was reached) followed by a blow to the head. The implant was then recovered and data downloaded. Four complete data sets (Fish 1, 3, 4 and 5) were obtained from the experiment. During data download, sampling bursts were concatenated into two continuous steady-state data sets where the first 15 min represented low current speed and the final 15 min represented high current speed. The middle 3 minutes (corresponding to 6 min in real time due to the duty cycling) were omitted to avoid the transient phase between the two speeds. Due to an unknown tag failure, one fish (Fish 2) provided only a partial dataset from the first 12 min of the experiment which after concatenation resulted in a 6 min data set.

2.5. Experiment 2

Experiment 2 was conducted using a Blazka swim respirometer (116 cm length X 24 cm diameter, 55 l volume) (Blazka et al., 1960) equipped with a temperature compensated dissolved oxygen sensor (NEOFOX, Ocean Insight, Duiven, The Netherlands).

Eight random fish (fork length 46.4 ± 1.1 cm, weight 1367 ± 130.0 g, Fulton's K-factor 1.4 ± 0.1) were captured from their holding tank using a knotless dip net and subsequently underwent the same protocol for surgically implanting the tags as described for Experiment 1. Each fish was implanted with a PO tag programmed with a 65 min start delay and a sampling frequency of 200 Hz. The tags were not set up with duty cycling and thus provided continuous data sets of 33 min. After surgery, the fish was placed inside the swim tunnel for wake-up. Swimming speed (i.e., water speed) inside the swim tunnel was set to $\approx$ 0 BLs^{-1} during this period.

During the wake-up period for each individual fish, 30 l sea water were deoxygenated by vigorous bubbling with instrument nitrogen (purity ≥99.9%) for ≥ 20 min. After the fish had woken from anesthesia, swimming speed was increased to 0.5 BLs^{-1} where it was kept for the remainder of the experiment. The tunnel remained connected to the same sea water supply as the holding tank until the logger started (i.e., about 65 min post tagging). The water supply was closed 3 min after logging had started, and the deoxygenated water pumped into the swim tunnel, thus abruptly reducing the dissolved oxygen in the tunnel to hypoxic levels. For the next 25 min, no water was replaced in the swim tunnel, effectually keeping the conditions hypoxic with fish respiration leading to a gradual decrease in the DO level from $\approx$ 5.5 mg L^{-1} to 3.8 mg L^{-1}. Five min before the experiment ended (i.e., 25 min after logging started), the valve to the water supply was reopened and fresh sea water exchange was resumed until logging was concluded at 33 min. Experiment 2 therefore consisted of three periods: Pre-hypoxia (3 min), hypoxia (25 min) and post-hypoxia (5 min).

Using this procedure, data were obtained for one control fish under normoxic conditions and seven test fish exposed to hypoxic conditions. The experiments for the control fish and test fish 2, 4, 5, 6, and 7 resulted in complete 33 min data sets. The experiment for Fish 3 resulted in a partial data set due to tag failure after 29 min. Although the experiment for Fish 1 resulted in a full 33 min data set, water circulation in the swim tunnel was restored $\approx$ 3 min later than dictated by the general procedure because of a valve issue during the trial for this fish. Thus the period of hypoxia was $\approx$ 27 min and the re-oxygenation period $\approx$ 1 min for this fish. It should also be noted that the DO sensor in the tunnel failed during the trial for Fish 7. However, since the test procedure was identical to that of all other fish, the DO profile in the tunnel was expected to be comparable to that of the other test fish. All individual fish were removed from the swim tunnel after their data logging periods had elapsed and immediately euthanized using the same method as in Experiment 1.

2.6. Data processing

To address the SpO_2 estimation challenge for Atlantic salmon, the proposed processing method is an adaptation of techniques used for human PPGs, and consists of four main steps: Preprocessing, ECG HR estimation, MA reduction and SpO_2 estimation (Fig. 1).

Preprocessing and HR estimation were applied to entire data series, while the remaining steps applied to 20 s processing windows with 15 s overlap. Details for each step are presented in subsequent sections. All data were processed using Anaconda's Python 3.8 distribution (Anaconda Inc., Austin, Texas, USA).

2.6.1. Preprocessing

Preprocessing involved applying a 3rd order Butterworth band-pass filter with passbands 0.2 Hz to 10 Hz for PPG and 5 Hz to 80 Hz for ECG. The cutoff frequencies were determined by considering the signal bandwidth in the frequency domain. PPG for both wavelengths was then scaled to $[0, 1]$ using

$$x_{scaled} = (b - a) \cdot \left(\frac{x_i - x_{min}}{x_{max} - x_{min}} \right) + a, \tag{1}$$

with $a = 0$ and $b = 1$ to reduce the likelihood of numerical instability during MA reduction.

2.6.2. ECG HR estimation

ECG HR estimation required processing steps to enhance the QRS complex to obtain the HR. ECG signal quality was evaluated by considering which of the categories 'Good', 'Acceptable' or 'Unacceptable' the raw signals fit into. This was similar to evaluations used for human ECGs for this purpose (van der Bijl et al., 2022). Generally, the ECG signals fit into the 'Good' and 'Acceptable' categories with only very few and short instances of 'Unacceptable' during the swim tunnel experiment where the fish exhibited temporary behavior which it would not express in other contexts outside the swim tunnel (e.g., trying to turn inside the tunnel). HR was obtained by applying the slope sum method (SSM) followed by the Teager–Kaiser instantaneous energy operator (TKEO) (Rankawat et al., 2015) to preprocessed ECG data. SSM involved taking the derivative of the ECG and summing only the positive derivative values over a time window matching the duration of the ECG QR slope. In this case, the time window was set to 0.02 s for all ECG data. TKEO involved calculating the instantaneous ECG energy, $\Psi[x(n)]$, by applying

$$\Psi[x(n)] = x^2(n) - x(n+1)x(n-1) \tag{2}$$

to the ECG data where $x(n)$ is the preprocessed ECG value at time $t = n$, followed by averaging within a 20 samples wide rolling window. ECG peaks were then detected and peak-to-peak time differencing was finally used to calculate the HR in Hz:

$$HR = \frac{1}{\Delta t}, \tag{3}$$

where Δt is the peak-to-peak time difference. An example of these processing steps is given in Fig. 2.

2.6.3. Motion artifact reduction

The MA reduction approach was based on the assumption that perfusion changes with the cardiac cycle (Yoshida et al., 2009; Svendsen et al., 2021c). Because ECG was available and the cardiac cycle correlates with PPG, a synthetic PPG reference was generated using ECG and its amplitude driven by the measured PPG, thus, enabling SpO_2 estimation. Because PPG signals are oscillatory in nature, a sinusoid

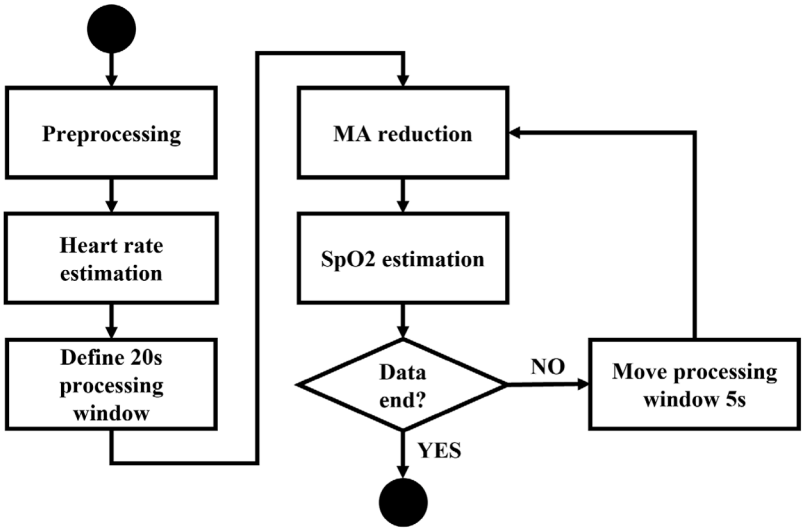

Fig. 1. Data processing main steps.

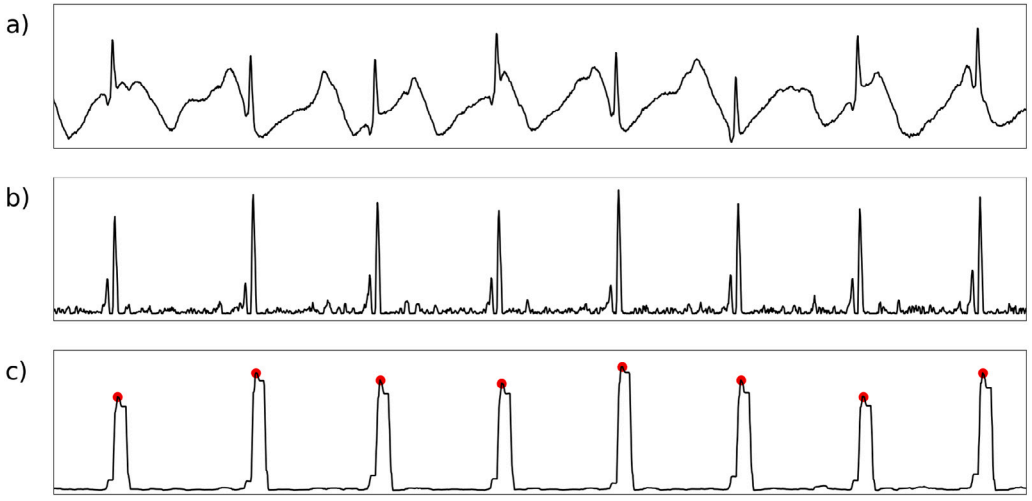

Fig. 2. Processing steps: (a) Raw ECG, (b) ECG after preprocessing and SSM, and (c) ECG after TKEO was applied and peaks detected (indicated with red dots).

matching the average HR was used as the synthetic PPG reference in each processing window. Thus,

$$ref = sin(2\pi \cdot HR_{avg} \cdot t_s). \tag{4}$$

In Eq. (4), HR_{avg} is the average ECG HR within a processing window and t_s the concurrent sampling time for both PPG and ECG.

The least mean squares (LMS) adaptive filter is a well established algorithm used to minimize the mean squared error between the filter's output and its desired response by adjusting its coefficients (Haykin, 2013) (Fig. 3).

The filter's intrinsic properties include independence on the reference phase and amplitude because only the error between the estimate ($y[k]$) and desired ($d[k]$) outputs are used to adjust the coefficients where the two correlate. In vector form, the LMS filter can be described as

$$y(k) = \mathbf{x}^T(k)\mathbf{w}(k), \tag{5}$$

where k is a discrete time index, $y(k)$ is the filtered signal, $\mathbf{w}$ is a vector of adaptive filter weights, and $\mathbf{x}$ is a vector consisting of the last n

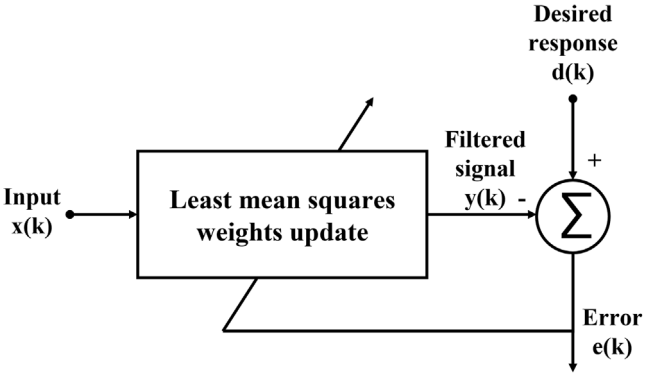

Fig. 3. LMS filter block general schematic.

samples of the input signal, defined by

$$\mathbf{x}(k) = [x(k), \ldots, x(k-n-1)]. \tag{6}$$

The weights, $\mathbf{w}$, are updated by

$$\mathbf{w}(k+1) = \mathbf{w}(k) + \Delta\mathbf{w}(k), \tag{7}$$

and $\Delta\mathbf{w}(k)$ is

$$\Delta\mathbf{w}(k) = \frac{1}{2} \cdot \frac{\delta e^2(k)}{\delta \mathbf{w}(k)} = \mu \cdot e(k) \cdot \mathbf{x}(k). \tag{8}$$

In Eq. (8), which represents a step in the steepest gradient search for the optimal filter weights, μ is the adaptation rate and $e(k)$ the LMS filter error defined by

$$e(k) = d(k) - y(k). \tag{9}$$

By considering the synthetic reference (Eq. (4)) as noisy in the sense that it lacks the features (i.e., amplitude change) required for SpO_2 estimation, it was set as the filter's desired output signal, $d(k)$, and the measured PPG as the filter input, $\mathbf{x}(k)$. Thus, the LMS algorithm imprints changes onto the synthetic PPG reference, $d(k)$, such that it correlates with the measurement, $x(k)$. Thus, the LMS adaptive filter is a suitable algorithm to drive the synthetic reference amplitude using the measured PPG. Data were processed using a filter width of $n = 40$ samples and a learning rate $\mu = 5 \cdot 10^{-4}$.

2.6.4. Scattering correction parameter

The starting point for deriving the scattering correction parameter, Γ, is the expression for SpO_2 that was estimated using the modified Beer–Lambert law,

$$A = \sum_i \varepsilon_\lambda \cdot C_i \cdot DPF_\lambda \cdot d, \tag{10}$$

where A is absorption, ε_λ chromophore $i's$ molar extinction coefficient for wavelength λ, DPF_λ the scattering-dependent differential path length factor for wavelength λ, and d the PO sensor's source-detector separation distance. SpO_2 is commonly expressed as the percent fraction of oxyhemoglobin (HbO) to total hemoglobin, $HbT = HbO + Hb$, where Hb is deoxygenated hemoglobin, so

$$SpO_2 = \frac{HbO}{HbO + Hb} \cdot 100\% = \frac{HbO}{HbT} \cdot 100\%. \tag{11}$$

By substituting Eq. (10) for two chromophores (HbO and Hb) into Eq. (11) and taking the ratio of two wavelengths to cancel unknowns, we arrive at an expression for SpO_2 that also includes $\Gamma = DPF_{\lambda 1}/DPF_{\lambda 2}$,

$$SpO_2 = \frac{\varepsilon_{Hb,\lambda 2} \cdot R \cdot \Gamma - \varepsilon_{Hb,\lambda 1}}{(\varepsilon_{HbO,\lambda 1} - \varepsilon_{Hb,\lambda 1}) - R \cdot \Gamma \cdot (\varepsilon_{HbO,\lambda 2} - \varepsilon_{Hb,\lambda 2})} \cdot 100\%, \tag{12}$$

where $\varepsilon_{HbO,\lambda 1}$, $\varepsilon_{HbO,\lambda 2}$, $\varepsilon_{Hb,\lambda 1}$ and $\varepsilon_{Hb,\lambda 2}$, are molar extinction coefficients that need to be set to proper values, and R is the modulation ratio,

$$R = \frac{max_{\lambda 1} - min_{\lambda 1}}{max_{\lambda 2} - min_{\lambda 2}}, \tag{13}$$

for PPGs normalized by their DC components (Nitzan and Taitelbaum, 2008; Kyriacou and Allen, 2021). Under the assumption that SpO_2 never exceeds 100% for individual fish, Eq. (12) can be solved for Γ resulting in

$$\Gamma = \frac{\alpha\varepsilon_{Hb,\lambda 1} + (\varepsilon_{HbO,\lambda 1} - \varepsilon_{Hb,\lambda 1})}{R_{min}(\varepsilon_{HbO,\lambda 2} - \varepsilon_{Hb,\lambda 2}) + \alpha\varepsilon_{Hb,\lambda 2}}, \tag{14}$$

where R_{min} is the smallest modulation ratio (Eq. (13)) in a data set and α is $100/SpO_2$. Eq. (14) was solved for $SpO_2 = 100\%$ for each data set (i.e., fish) from Experiment 1. The average of all correction parameters, Γ_{avg}, was then used during subsequent SpO_2 estimations.

2.6.5. SpO_2 Estimation

Because Atlantic salmon hemoglobin has absorption characteristics similar to human hemoglobin (Svendsen et al., 2023), the molar extinction coefficients needed in Eq. (12) were set to $\varepsilon_{HbO,\lambda 1} = 319.6$, $\varepsilon_{HbO,\lambda 2} = 1154.0$, $\varepsilon_{Hb,\lambda 1} = 3226.56$ and $\varepsilon_{Hb,\lambda 2} = 726.44$, respectively (Prahl, 1998). When solving Eq. (12), the average modulation ratio within a 20 s processing window was used for R and Γ_{avg} obtained using Eq. (14) for Γ. Finally, the SpO_2 results were smoothed using a 3rd order Butterworth low pass filter with a cutoff frequency of 0.02 Hz. The initial 30 s of data after filtering were omitted due to the filter's settling time.

2.6.6. Result interpretations

For Experiment 1 it was hypothesized that SpO_2 estimated using Γ_{avg} would remain within the expected range of 95% to 100% for both water current speeds. The data were tested for normality by using quantile–quantile (Q–Q) analysis (Ghasemi and Zahediasl, 2012). For each data set, outliers were removed by calculating the z-score of each value relative to the sample mean and standard deviation. Data points with a z-score greater than ±3 were labeled as outliers and removed. The mean and 95% confidence intervals for each data set were then calculated and evaluated with respect to the expected range.

For Experiment 2 it was hypothesized that the relative SpO_2 difference during hypoxia would be greater compared to pre and post hypoxia periods because each fish had to adapt to the changing conditions. Because physiological response depends on the (physiological) state of each individual and, in this case, residual effects expected from anesthesia and surgery, data was not assumed to be normally distributed in any of the experiment periods. This assumption was supported by Q–Q analysis where sample quantiles did not align well with the theoretical quantiles for a normal distribution. For Experiment 2, the relative SpO_2 differences and medians were therefore calculated separately for each period and compared.

3. Results

The results show that PPG for 660 nm and 880 nm could be successfully measured. Both the long term trend (i.e., baseline) and the high frequency variations caused by blood circulation were visible (Fig. 4).

All data sets from both experiments featured typical PPG traits such as saliency, baseline wandering, hyperperfusion events and MA (Figs. 5 and 6).

The measured PPGs could be divided into three categories: 'salient', 'MA corrupted' and 'bad' (Fig. 6). In general, the measured PPGs were in the 'salient' and 'MA corrupted' categories with sporadic instances of the 'bad' category. PPGs in the 'bad' category were coincident with high activity events such as burst swimming in Experiment 1 and flight responses in Experiment 2. The LMS algorithm successfully tracked 'salient' PPGs and reconstructed saliency for 'MA corrupted' signals. In the case of 'bad' PPGs no clear pulsatile component concurrent with HR was present. Thus, the correlation with the synthetic reference was too low for successful filtering by the LMS algorithm.

3.1. Experiment 1

The MA compensated data from Experiment 1 allowed an estimation of the average scattering compensation parameter using Eq. (14) for low ($\Gamma_{avg,low} = 0.33$) and high ($\Gamma_{avg,high} = 0.37$) water currents, resulting in an average scattering correction parameter of $\Gamma_{avg} = (\Gamma_{avg,low} + \Gamma_{avg,high})/2 = 0.35$ (Table 1).

Using Γ_{avg} in Eq. (12) for all data obtained from Experiment 1 resulted in average SpO_2 values of 96.98±0.08 and 96.44±0.09 calculated for low and high water current speeds, respectively. Both means and confidence intervals were within the expected SpO_2 range of 95% to 100% for both water currents (Table 2).

The average relative SpO_2 differences (max–min) for low and high water current were 2.42% and 2.87%, respectively (Table 2).

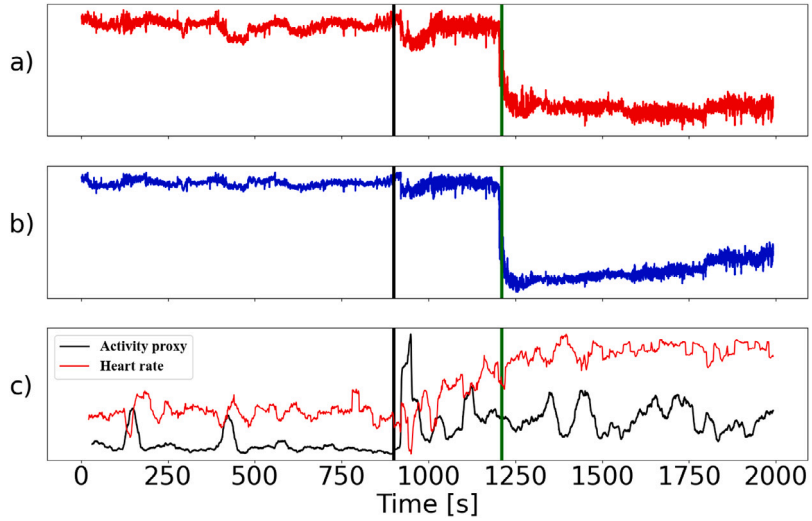

Fig. 4. Raw PPG data from one exemplary fish for (a) 660 nm and (b) 880 nm from Experiment 1. An acceleration based activity proxy (black) and HR (red) are shown in (c). The black vertical line denotes the time when the water current speed was increased, and the green vertical line indicates a hyperperfusion event (i.e., increased perfusion). Note the increase in amplitude after water current speed was increased which coincided with the higher activity levels seen in (c).

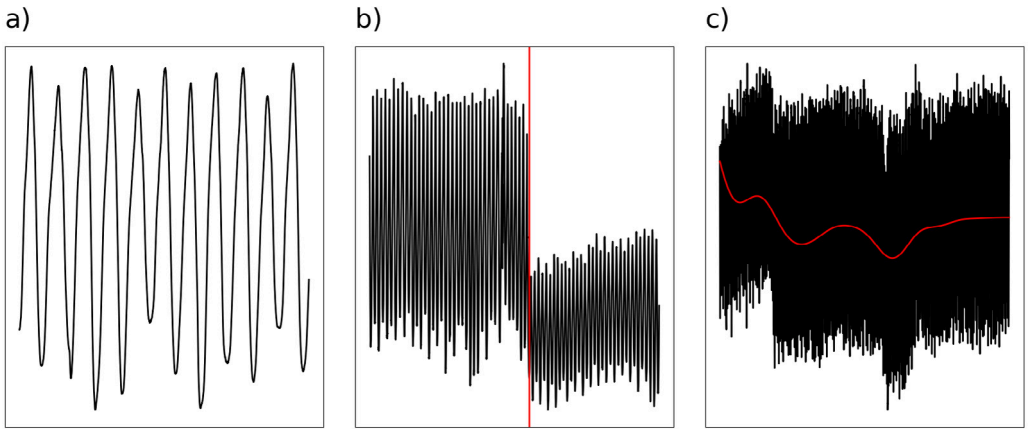

Fig. 5. Examples of typical PPG traits such as saliency (a), hyperperfusion event (b), indicated by the vertical red line and baseline wandering (c) identified in the measured data from Fish 2 in Experiment 2.

Table 1
Individual and average scattering compensation parameter Γ at high and low current speed, respectively, from Experiment 1.

	Fish 1	Fish 2	Fish 3	Fish 4	Fish 5	Average
Low speed	0.31	0.34	0.31	0.35	0.36	0.33
High speed	0.33	–	0.38	0.41	0.41	0.37

3.2. Experiment 2

Using the MA compensation approach and the average scattering coefficient obtained in Experiment 1 (Γ_{avg}), a median SpO_2 of 100.70%, and a min–max variation of 4.53% was calculated for the entire data set for the control fish. For the test fish, the average median SpO_2 before, during, and after hypoxia was 97.18% for the pre hypoxia period, 97.27% for the hypoxia period and 97.43% for the post hypoxia period (Table 3). The corresponding average relative SpO_2 differences (max–min) were 2.41% pre hypoxia, 4.75% during hypoxia, and 2.25% post hypoxia (Table 4).

All test fish had a larger relative difference in SpO_2 during the hypoxia period compared to the pre and post hypoxia periods. This indicates that the PPG was affected by changes in dissolved oxygen, manifesting as observable changes in the SpO_2 estimate. Test fish 1–6 were able to maintain a median SpO_2 value within the expected SpO_2 range at all times. For fish 7, the same applied to the pre hypoxia and hypoxia periods, while the SpO_2 estimate just exceeded 100% for the post hypoxia period. The average relative change for the test fish was 0.22% higher during the hypoxia period compared to the relative change calculated for the control fish but with individual differences up to 2.6%. Additional plots and evaluations for each fish from Experiment 2 are given in Appendix.

4. Discussion

In this pilot study for PO in Atlantic salmon, PPG and ECG data were successfully collected under normoxic and hypoxic conditions. Using these data, a viable MA compensation approach was derived and an average scattering compensation parameter calculated. Based on these results, PPGs measured under normoxic conditions resulted in an SpO_2 estimate within the expected range, while PPGs measured under hypoxic conditions showed that the PO sensor responded to changes in SpO_2. The experiments can thus be considered successful.

The relative SpO_2 difference from Experiment 1 were greater for high compared to low water currents which may indicate greater impact from MA for high compared to low water current. This is supported by both activity proxies and video material for the experiment which

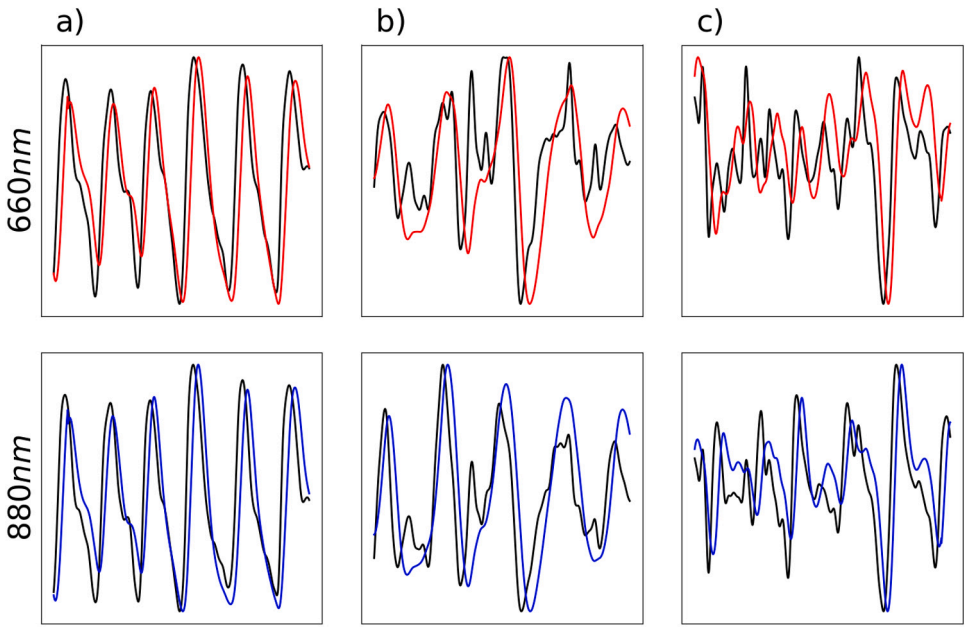

Fig. 6. Examples of (a) a salient PPG, (b) a MA corrupted PPG, and (c) a bad PPG. In all plots the black line depicts the preprocessed PPG, while the colored line depicts the LMS filtered (i.e. MA compensated) PPG.

Table 2
Absolute $SpO_2 \pm 95\%$ confidence interval and relative differences (ΔSpO_2) for all fish at high and low current speeds. for all fish at high and low current speeds. Due to tag failure, low speed data duration for Fish 2 was 6 min. High speed data was not available for Fish 2.

	Fish 1	Fish 2	Fish 3	Fish 4	Fish 5	Average
Low speed	96.56 ± 0.08	97.23 ± 0.06	97.43 ± 0.07	97.00 ± 0.04	96.68 ± 0.15	96.98 ± 0.08
High speed	96.34 ± 0.09	–	97.17 ± 0.09	96.94 ± 0.02	95.32 ± 0.14	96.44 ± 0.09
Low speed ΔSpO_2	2.41	0.63	3.13	1.30	4.64	2.42
High speed ΔSpO_2	2.91	–	2.53	1.43	4.60	2.87

Table 3
Median and average values for the pre hypoxia, hypoxia and post hypoxia periods.

	Fish 1	Fish 2	Fish 3	Fish 4	Fish 5	Fish 6	Fish 7	Average
Pre hypoxia median	95.17	96.15	97.77	96.06	97.36	98.68	99.25	97.18
Hypoxia median	94.96	96.88	97.94	95.75	99.24	99.24	99.91	97.27
Post hypoxia median	95.41	97.10	97.95	96.73	97.18	97.18	100.47	97.43

Table 4
Relative differences in estimated SpO_2 between the pre hypoxia, hypoxia and post hypoxia periods for the fish subjected to hypoxic conditions.

	Fish 1	Fish 2	Fish 3	Fish 4	Fish 5	Fish 6	Fish 7	Average
Pre hypoxia	5.10	1.84	1.07	2.69	2.20	2.01	1.97	2.41
Hypoxia	6.66	4.58	3.04	5.26	7.15	3.47	3.08	4.75
Post hypoxia	2.87	1.97	0.72	2.39	3.54	3.19	1.04	2.25

document intermittent swimming bursts after water current speed was increased and the fish had to re-establish their positions in the tank (Fig. 4(c)). The absolute values, however, were all within the expected range of 95% to 100% (Table 2). It is thus considered likely that the methods used to estimate SpO_2 gave reasonable results.

For Experiment 2 the estimated SpO_2 consistently showed greater variation during hypoxia period compared to the pre and post hypoxia periods (Table 3). This was as expected since the fish had to adapt to the hypoxic conditions through behavioral and physiological adjustments to maintain median levels. Because the combined time for surgery and recovery was limited to 65 min for the swim tunnel, the control for Experiment 2 was included to get an impression of whether or not the SpO_2 estimate resulted in expected values. The relative difference and median for the control indicate that the fish recovered sufficiently for the technology test in this pilot study.

During Experiment 1, data were collected from five Atlantic salmon under normoxic conditions with the aim to find an average scattering compensation parameter and an MA compensation approach using an LMS filter with a synthetic PPG reference constructed using ECGs collected intraperitoneally. This is considered valid because PPG correlates with the cardiac cycle (Yoshida et al., 2009; Svendsen et al., 2021c). Intraperitoneal ECG collection is the most common way to obtain HR from free swimming fish, and the measured ECGs were generally of 'Good' and 'Acceptable' signal quality. Short instances of 'Unacceptable' signal quality were recorded when the fish exhibited behavior which it would not express outside a swim tunnel. The effect of these instances were mitigated by HR averaging within a processing window.

For Experiment 1 it was assumed that SpO_2 for all individuals would be 100% due to the normoxic conditions. This assumption is supported by e.g., Steinhausen et al. (2008) and Clark et al. (2008) who reported that species comparable to Atlantic salmon (Sockeye Salmon (*Oncorhynchus nerka*) and Chinook salmon (*Oncorhynchus tshawytscha*)), have PaO_2 at rest of 97 Torr and 90 Torr, respectively which corresponds to $\approx$ 100% SpO_2 (Madan, 2017). Using the MA compensated PPGs and Γ_{avg} in Eq. (12), the resulting SpO_2 estimates for the fish in Experiment 1 were within the expected range of 95% to 100%.

Although the implantation procedure and tag placement were similar for all fish, individual differences in anatomy and tissue composition within the sensing volume mean an average value for scattering compensation ($\Gamma_{avg} = 0.35$) introduces an inaccuracy when calculating SpO_2 using Eq. (12) which may result in values exceeding 100%. This effect is similar to that arising from empirical mapping procedures in human PO. Note, however, that values in Table 1 are quite similar for

low and high speeds. This indicates that PPG sensing conditions were comparable between individuals. The calculated values for Γ were, however, consistently higher for high compared to low water speed. One possible explanation for this could be that the increased swimming speed resulted in increased blood pressure and tissue perfusion, thus affecting sensing conditions (e.g., light back scattering). This is supported by increased PPG amplitude (associated with blood pressure) and a decrease in PPG mean (associated with increased perfusion) observed in raw data for all fish in Experiment 1 (Fig. 4). PPG decreases when perfusion increases due to greater light scattering and absorption, thus, reducing the amount of light reaching the photo detector. These elements indicate that the PO measured a PPG (as opposed to pure MA noise), and that the MA compensation approach and the average scattering compensation parameter were valid and could be used for SpO_2 estimation.

In Experiment 2, Atlantic salmon were implanted with the aim to see if the PO sensor would respond to changes in SpO_2 using the methods and results from Experiment 1. To this end, individual implanted fish were consecutively placed in a swim tunnel and subjected to hypoxic conditions (down to $3.8\,\mathrm{mg\ L^{-1}}$). At such levels, hypoxic responses have been observed previously in Atlantic Salmon (Vikeså et al., 2017; Remen et al., 2016) suggesting that reduced arterial SpO_2 may be observed (Farrell and Richards, 2009). Thus, SpO_2 was expected to vary between individuals during the hypoxia period as observed.

The data processing methods were inspired by approaches for MA detection and removal in human PPGs using synthetic Refs. Lim et al. (2018) and Shin et al. (2021). These approaches rely on widely accepted PPG morphology. Although the measured PPGs generally show typical PPG traits such as saliency, hyperperfusion events, and baseline wandering (Fig. 5) (Park et al., 2022), accurate knowledge of fish PPGs is currently limited. Such variations may be caused by anatomical differences and circulatory function. For instance, Atlantic salmon has a secondary, low pressure, circulatory system (Bone and Moore, 2008). Any difference in pulse transit time (PTT) for arterial blood between the two circulatory systems can for the same cardiac cycle change the PPG shape because the (arterial) blood arrives in the sensing volume at different times.

The MA reduction method was successful in most situations when the PPG signal was not extremely distorted and had a clear pulsatile component. However, the variability between cases yielding valid PPG signals (e.g., Fig. 6(a) vs. (b)) seems to be much higher compared to valid human PPGs, implying a greater variation in PPG morphology may have to be accepted for fish compared to humans when estimating both HR and SpO_2. It is likely that this approach will not be equally effective when the pulsatile component is not equally clear. For example, the data shown in Fig. 6(c) were obtained during Experiment 1 where a fish showed momentary intensive burst swimming. This implies that the filtering/MA reduction approach cannot be expected to work well in all instances where the fish exhibits abrupt changes in movement. Thus, the LMS approach may be limited to MAs that are not so large that they effectually override any pulsatile components in the signal, and thus remove the ability to correlate this with the reference. However, in such cases it can be expected that the MAs are distinct from the PPG in the time/frequency domains and can then be compensated for by constructing a suitable MA reference using the 9-axis inertial motion unit which is part of the PO tag. Such an approach, combining both the synthetic PPG reference presented in this study with conventional acceleration based approaches, should be a subject in future work.

The SpO_2 processing method required that an accurate HR estimate could be obtained using ECG for a valid synthetic reference. Although ECG was susceptible to motion (though less than PPG), SSM and TKEO are methods suited to enhance peaks in noisy signals (Rankawat et al., 2015) and generally performed well for the purposes of this pilot study, as seen in Fig. 2. In some cases in Experiment 2, motion affected ECG in a way that made peak detection challenging. Such periods may have been caused by abrupt changes in movement momentarily changing the ECG sensing conditions. They were, however, of limited duration and their effects were alleviated by averaging. The synthetic reference consisted of a sinusoid with a frequency matching the average HR within a processing window (lasting 20 s with a 15 s overlap with the previous window). These values were chosen because a window $< 20\,\mathrm{s}$ increased the likelihood of numerical instability in the LMS filter and generally resulted in increased noise, likely due to reduced averaging effect in the SpO_2 estimate. Similarly, a window $> 20\,\mathrm{s}$ reduced performance of the LMS filter because HR is likely to change over time. The average HR may thus not correlate sufficiently with the PPG using longer windows. The overlap of 15 s was chosen to minimize this effect. Additionally, the 15 s overlap was motivated by the lowest expected HR of 15 BPM for Atlantic Salmon (Lucas, 1994) and comparable species (Brijs et al., 2019), i.e., one heart beat every 4 s. To allow for some margin for new data to be included within the processing window and to obtain a reasonable data resolution, the overlap was set to 15 s, thus giving one SpO_2 estimate every 5 s.

Because the SpO_2 estimate is driven by the modulation ratio (Eq. (13)) the reference did not have to be an exact morphological PPG duplicate as long as its amplitude was driven by correlation with the measured PPG in the LMS filter. Since perfusion is concurrent with the cardiac cycle, a sinusoid with a frequency matching the HR was considered a feasible choice. Note, however, that this approach could also be a source of error if the HR changes considerably within a processing window. In such instances the difference between the average HR used for the synthetic reference and the instantaneous HR will affect the correlation between the measured signal and the reference used by the LMS filter, thus reducing its performance. Future implementations may employ more sophisticated approaches such as template matching to address this challenge if an accepted PPG shape for Atlantic salmon becomes available.

Tissue composition and their optical properties within the PPG sampling volume are important when estimating SpO_2. Due to individual differences in anatomy it is prudent to consider whether sensor placement could have had an impact on the data. The link between the estimated SpO_2 values and ambient DO-conditions appeared to be stronger for some fish (e.g., Fish 5 in Experiment 2 (Table 3)) compared to others. An explanation for such differences may be salmon's capabilities compensate for reduced DO through physiological mechanisms that increase their ability to absorb O_2 from the water (e.g., increased gill area and ventilation frequency, increased HR and/or stroke volume), or mechanisms reducing their consumption of O_2 (e.g., reduced activity). This could also explain some of the larger inter-individual variations seen during the hypoxic periods as the above mentioned mechanisms can take some time before being properly activated, and that different individuals could have different tolerance limits at which such mechanisms will be necessary.

While the results show that it is possible to estimate SpO_2 in free-swimming salmon, they also imply that Atlantic salmon are resilient with respect to temporary hypoxia due to their various coping mechanisms. Exploring the potential effect of such mechanisms and their role in maintaining homeostasis would require further trials, where the fish could be kept at lower DO levels over longer times as this could identify when these mechanisms are no longer sufficient to prevent physiological breakdown. However, conducting such experiments would be both complex and difficult to do properly, as well as being ethically challenging.

5. Future work

While the results from this pilot study indicate that SpO_2 can be estimated for Atlantic salmon, future work aimed at exploring ways to further improve the accuracy and reliability of the estimates could strengthen the potential of this method in monitoring the physiological status of farmed fish. As mentioned, the MA compensation works

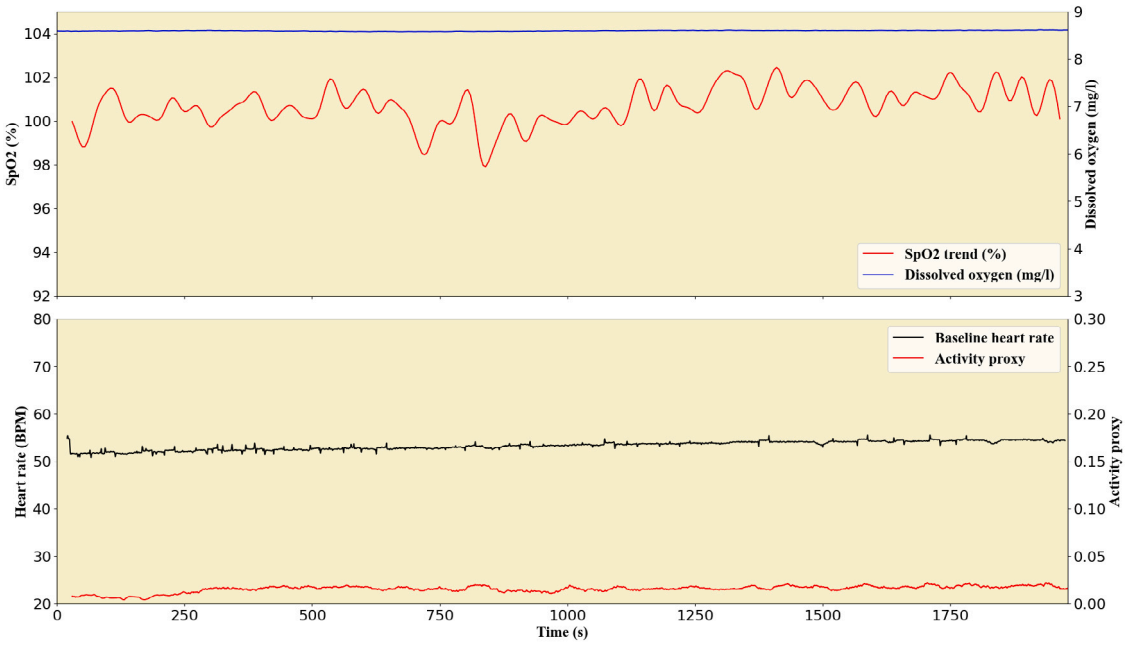

Fig. 7. Experiment 2 - Control.

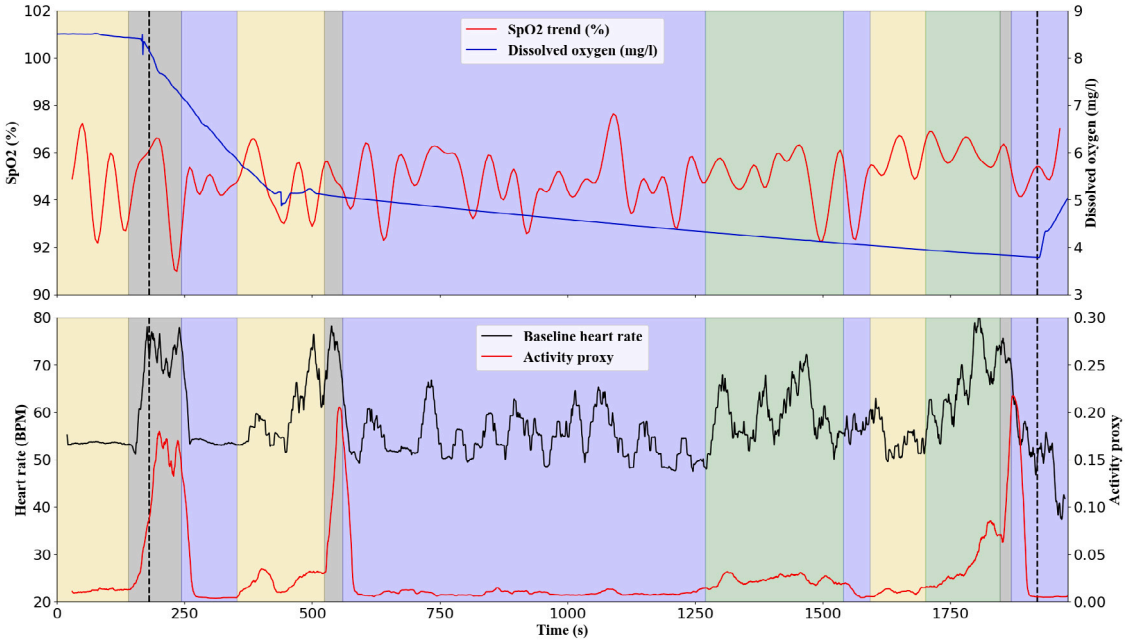

Fig. 8. Results for Fish 1.

for cases where a synthetic reference can be constructed using ECG. Because the PO implant also contains an inertial motion unit, MA compensation could be enhanced by combining the current method with motion data for improved and robust MA compensation and PO in Atlantic salmon.

Although these experiments have proven the concept of using such sensors to monitor fish, it is possible to further strengthen this conclusion by increasing the number of fish to allow sufficient statistical power for evaluations of statistical significance. This would require that authorities allow more effective measures to rapidly and reliably deoxygenate arterial blood (e.g., carbon monoxide exposure).

SpO_2 estimation accuracy may further benefit from additional validation studies combining implantation with dorsal aorta (DA) cannulation in controlled raceway/swim tunnel trials. Since DA cannulation enables blood gas analysis simultaneous with measurements acquired with the implant, this would provide a more accurate SpO_2 baseline for comparison.

The PPGs measured in the experiments show traits (e.g., PPG amplitude and hyperperfusion events) which in humans are associated with changes in cardiac output (CO), the product of stroke volume and HR. It is believed that fishes actively adjust their heart's stroke volume by the Frank-Starling mechanism (Tota et al., 2005). It has also been shown that stress response is associated with HR (Svendsen et al., 2021a). Because the ability to deliver oxygen to tissues depends on CO, it is possible that using HR as a stress indicator alone is inaccurate if the fish simply compensates by adjusting CO. This may offer an explanation the drop in PPG mean without a concurrent increase in HR as seen in Fig. 4 which indicates that the fish increased the stroke volume of its

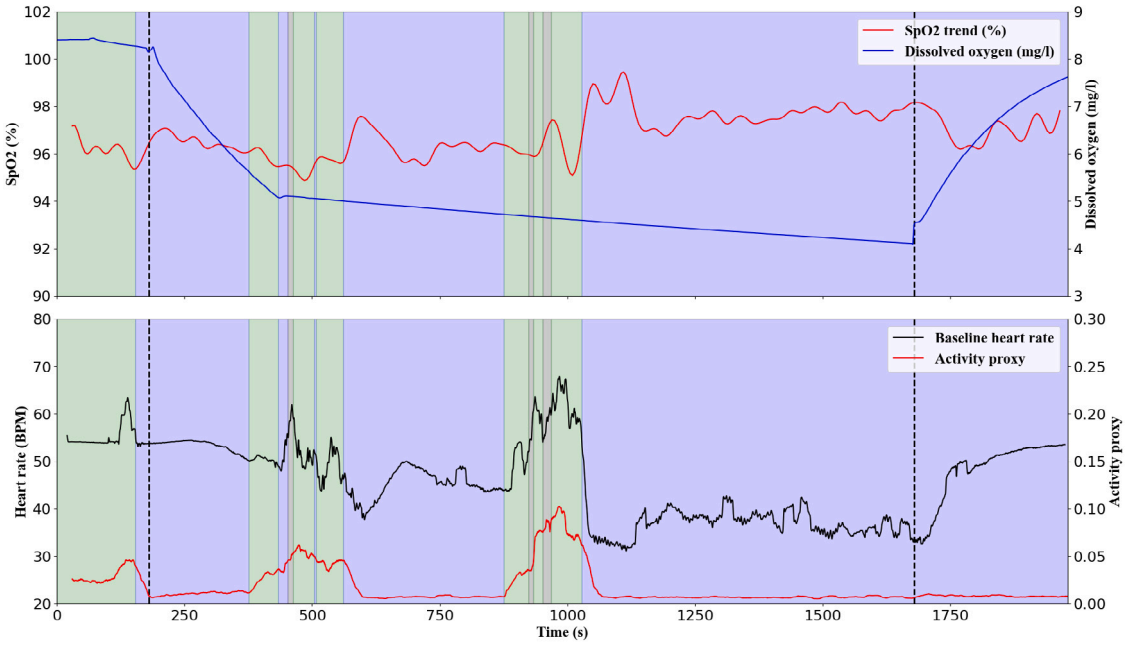

Fig. 9. Results for Fish 2.

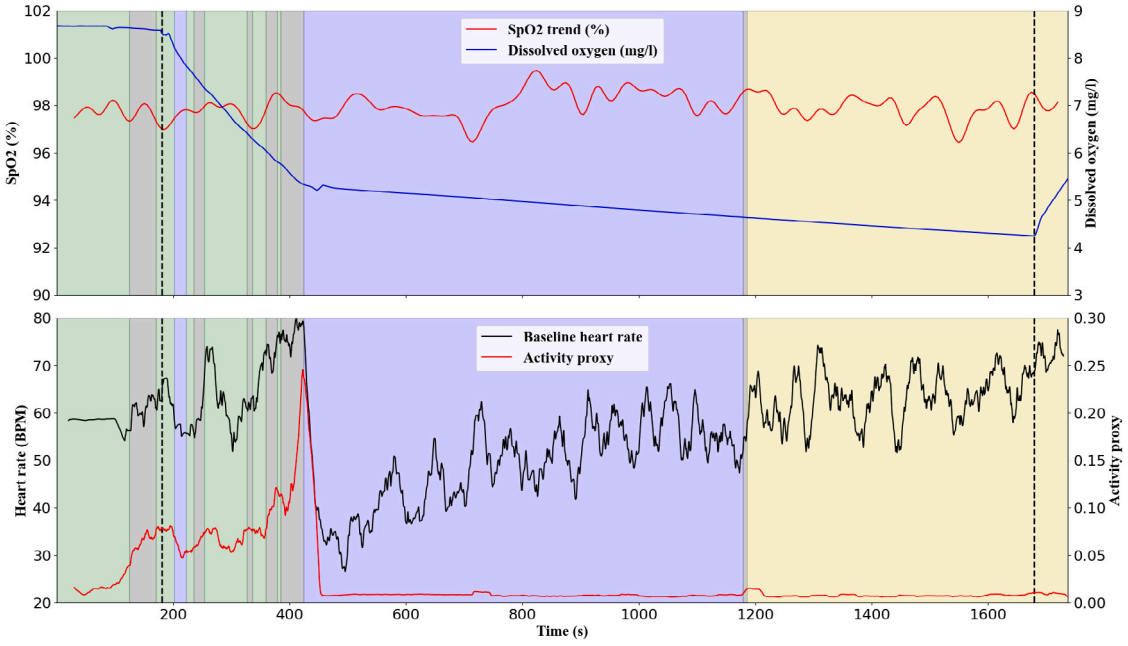

Fig. 10. Results for Fish 3.

heart to increase perfusion. Thus, PPG measurements with appropriate signal processing open the possibility to evaluate stress levels in terms of both HR and CO evaluations.

ECG was also affected by MA, thus challenging the accuracy of the synthetic reference. Combining SSM and TKEO resulted in a powerful tool to enhance the QRS complex in preprocessed ECG signals (Fig. 2), but robustness may in the future be improved by implementing scaling and a more sophisticated peak detection approach after TKEO.

6. Conclusion

The results from this pilot study show that PPG from free swimming Atlantic salmon can be collected using an implanted PO tag. Although PPGs were affected by MA, a filtering approach using a synthetic PPG reference and a LMS filter were successfully derived and used for compensation. Because alternative calibration techniques were unavailable for fish, a light scattering compensation parameter was calculated under the assumption that SpO_2 was 100% for fish under normoxic conditions. Using MA and light scattering compensation, values for SpO_2 within the expected range were calculated for all experiment fish. It is therefore considered that SpO_2 can be an addition to the selection of physiological response parameters possible to measure using implants. If PO implants can be adapted as part of future Atlantic salmon farming (e.g., in the form of sentinel fish Føre et al., 2017a), producers may obtain additional objective data providing insight into the physiological state of the biomass. This can, in turn, contribute to improved animal health and welfare.

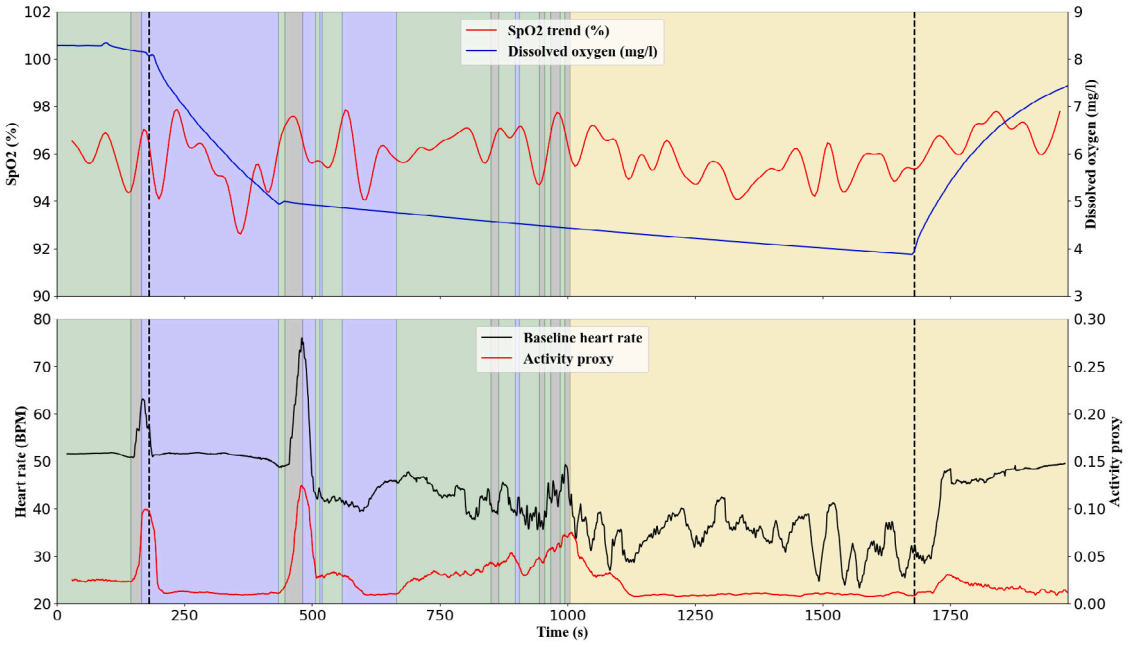

Fig. 11. Results for Fish 4.

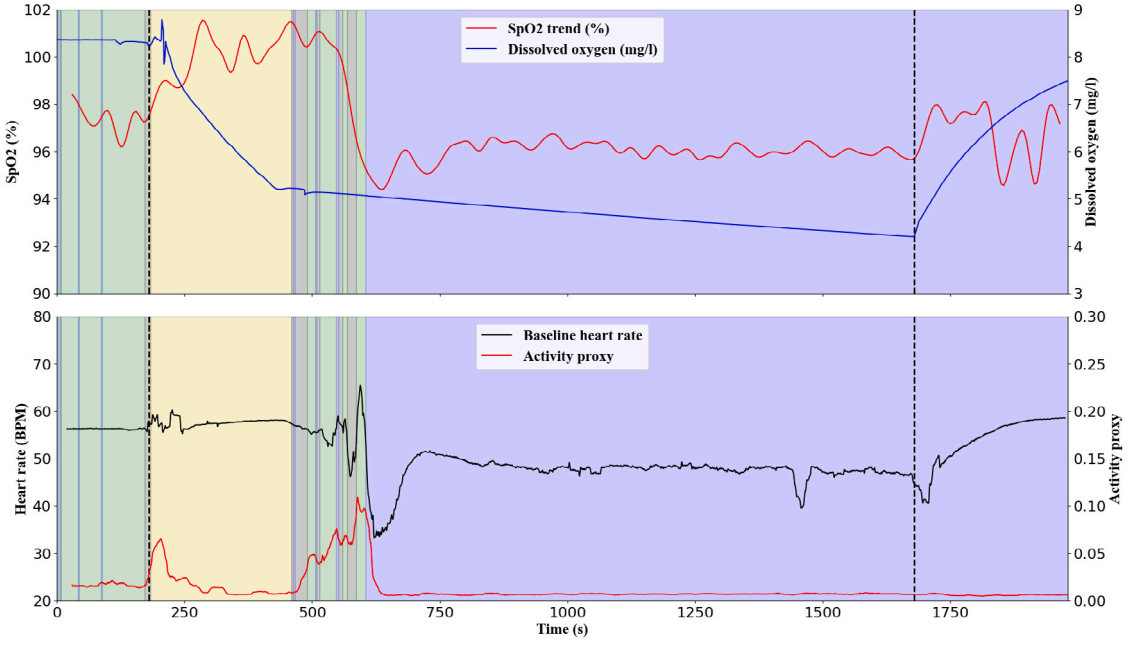

Fig. 12. Results for Fish 5.

CRediT authorship contribution statement

E. Svendsen: Method development, Data curation, Writing – original draft. **M. Føre:** Method development, Writing – original draft. **L.L. Randeberg:** Method development, Writing – original draft. **R.E. Olsen:** Writing – original draft. **B. Finstad:** Writing – original draft. **M. Remen:** Writing – original draft. **N. Bloecher:** Writing – original draft. **J.A. Alfredsen:** Method development, Writing – original draft.

Declaration of competing interest

The authors declare that they have no known competing financial interests or personal relationships that could have appeared to influence the work reported in this paper.

Data availability

Data will be made available on request.

Appendix

In this appendix data from each individual fish used in Experiment 2 are presented and discussed. Because MA is caused by activity, the common activity proxy using the 30 s rolling mean of the acceleration norm commonly found in literature (e.g., Svendsen et al., 2021a) was calculated for co-evaluation with SpO_2 and the baseline HR used for the synthetic PPG reference. In all figures, the colored background denotes different behaviors with green being swimming, yellow being burst and glide (glide period $\leq$ 5 s), blue is station keeping and gray

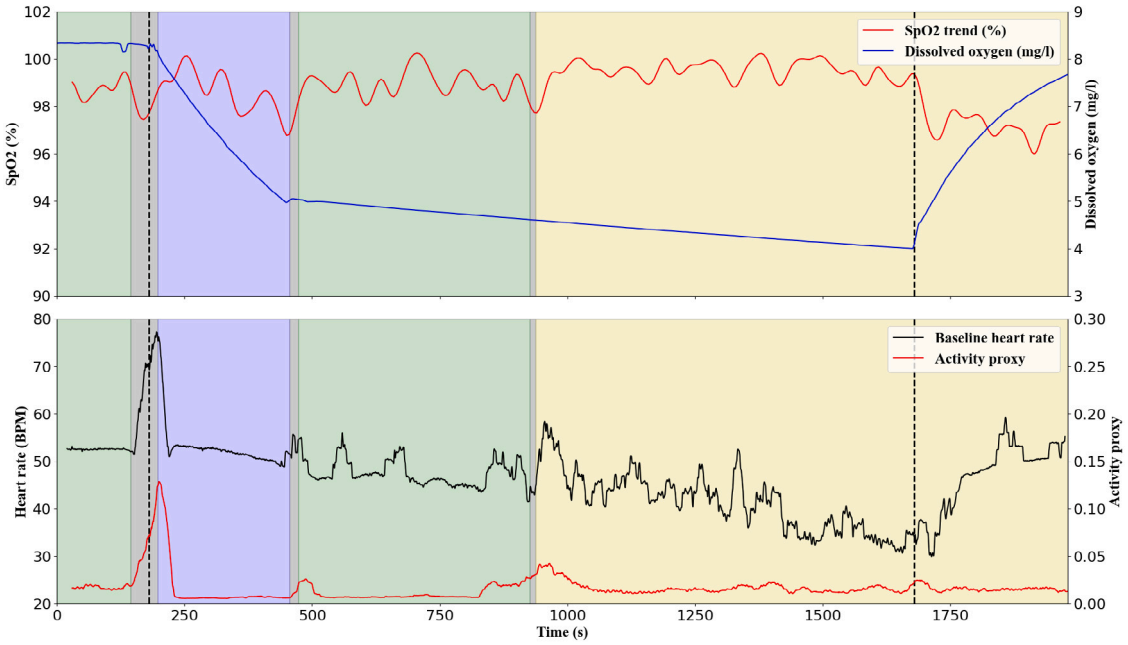

Fig. 13. Results for Fish 6.

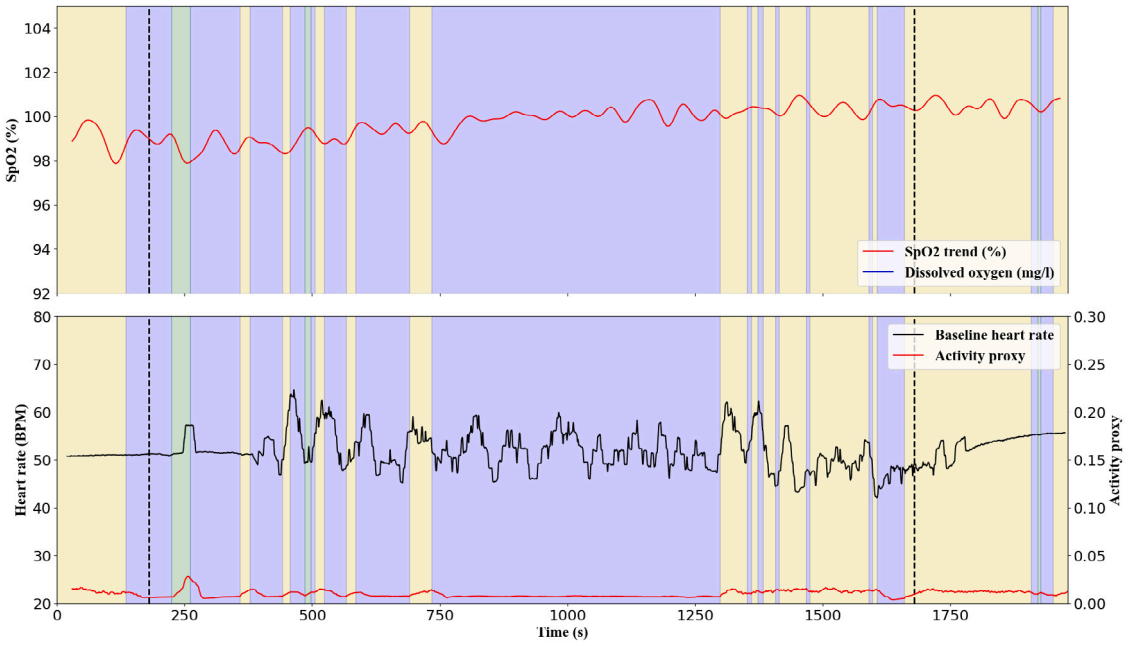

Fig. 14. Results for Fish 7.

is high activity periods with behavior not falling into any of the other categories. In the figures below, the vertical dotted lines, where present, indicate the hypoxia period.

Control

The control exhibited the same behavior and stable HR throughout the entire duration of the trial. SpO_2 was stable showing little change as can be expected under normoxic conditions. Note that SpO_2 is high and sometimes more than 100%. This is caused by using an average value for scattering compensation which will introduce an estimation inaccuracy for individuals (see Fig. 7).

Fish 1

Measurements for Fish 1 resulted in a complete 33 min data set. Compared to the other fish, the hypoxia period was ≈ 3 min longer due to an unforeseen valve issue. Fish 1 was generally able to maintain SpO_2 with the exception of transient reductions during high activity periods. During periods of station keeping the SpO_2 level is restored, likely due to reduced demand (see Fig. 8).

Fish 2

Measurements for Fish 2 resulted in a complete 33 min data set. Fish 2 was generally able to maintain SpO_2 throughout the hypoxic period,

with the exception of transients during periods of high activity. The high activity periods are followed by a period of reduced activity during which SpO_2 is restored or even increased. These results may reflect successful compensation during a period of reduced oxygen availability, e.g. by increasing gill ventilation and perfusion (Perry et al., 2009) (see Fig. 9).

Fish 3

Measurements for Fish 3 resulted in a 29 min data set, i.e, 4 min shorter compared to the other data sets to tag failure. Thus, the post hypoxia period was only 1 min for Fish 3. During hypoxia Fish 3 is able to maintain SpO_2, also during and following a period of high activity as oxygen is reduced from > 8 mg/l to approximately 5.5 mg/l. This indicates that compensatory responses (e.g. increased gill ventilation and perfusion) successfully upholds oxygen uploading at the gills, also during a period of high activity, possibly as a response to the declining DO. The reduced HR and activity that follows after the activity burst, at low DO, may indicate a post exercise oxygen demand that results in functional hypoxia and bradycardia (reduced HR and increased stroke volume Farrell and Richards, 2009) (see Fig. 10).

Fish 4

Measurements for Fish 4 resulted in a complete 33 min data set. Fish 4 was generally able to maintain SpO_2 with the exception of a transient increase during a period with stable swimming activity when the hypoxia period starts. Fish 4 was quite active during the trial, and together with the maintained SpO_2, this may indicate successful compensation during a period with lowered oxygen availability (see Fig. 11).

Fish 5

Measurements for Fish 5 resulted in a complete 33 min data set. The results show interesting and distinct SpO_2 responses. Of note is the first major SpO_2 drop after a period of increasing activity, when DO declines and reaches approximately 5 mg/l. After this, SpO_2 remains lower than in the pre-hypoxia and post-hypoxia periods. Coincident with the drop in SpO_2, the HR dropped, first to low, then to intermediate levels compared to normoxia. These results may indicate that the individual first responded behaviorally to the declining DO (flight response), after which the post-exercise oxygen demand induced functional hypoxia and bradycardia. With DO levels between 4 and 5 mg/l in the hypoxic period, this individual was not able to successfully re-establish normoxic SpO_2 and HR before oxygen levels where increased (see Fig. 12).

Fish 6

Measurements for Fish 6 resulted in a complete 33 min data set. Fish 6 was generally able to maintain SpO_2 with exception of a transient increase during a low activity period when the hypoxia period starts. Fish 6 was quite active during the trial. Combined with SpO_2 results, this may indicate successful compensation during the hypoxic period (see Fig. 13).

Fish 7

Measurements for Fish 7 resulted in a complete 33 min data set. The DO sensor failed during the trial for Fish 7, thus, DO data are not available for this individual. The procedure for this fish was, however, identical to the other fish, so it was expected that the DO profile for Fish 7 was comparable to the other fish. Fish 7 was generally able to maintain and even increase SpO_2 during the trial. Fish 7 was not very active during the trial. This could indicate that oxygen availability and oxygen uptake was sufficient to fulfill the oxygen demand, possibly through compensatory responses such as increased ventilatory effort (see Fig. 14).

References

Aoyagi, T., 2003. Pulse oximetry: its invention, theory, and future. J. Anesth. 17 (4), 259–266.

Baktoft, H., Gjelland, K.Ø., Økland, F., Thygesen, U.H., 2017. Positioning of aquatic animals based on time-of-arrival and random walk models using YAPS (Yet Another Positioning Solver). Sci. Rep. 7 (1).

Blazka, P., Volf, M., Cepela, M., 1960. A new type of respirometer for the determination of the metabolism of fish in an active state. Physiol. Bohemoslov. 9 (6), 553–558.

Bone, Q., Moore, R., 2008. Biology of Fishes. Taylor & Francis.

Brijs, J., Sandblom, E., Axelsson, M., Sundell, K., Sundh, H., Huyben, D., Broström, R., Kiessling, A., Berg, C., Gräns, A., 2018. The final countdown: Continuous physiological welfare evaluation of farmed fish during common aquaculture practices before and during harvest. Aquaculture 495, 903–911.

Brijs, J., Sandblom, E., Rosengren, M., Sundell, K., Berg, C., Axelsson, M., Gräns, A., 2019. Prospects and pitfalls of using heart rate bio-loggers to assess the welfare of rainbow trout (Oncorhynchus mykiss) in aquaculture. Aquaculture 509, 188–197.

Casson, A.J., Galvez, A.V., Jarchi, D., 2016. Gyroscope vs. accelerometer measurements of motion from wrist PPG during physical exercise. ICT Express 2 (4), 175–179.

Chan, E.D., Chan, M.M., Chan, M.M., 2013. Pulse oximetry: understanding its basic principles facilitates appreciation of its limitations. Respir. Med. 107 (6), 789–799.

Clark, T.D., Sandblom, E., Cox, G.K., Hinch, S.G., Farrell, A.P., 2008. Circulatory limits to oxygen supply during an acute temperature increase in the Chinook salmon (oncorhynchus tshawytscha). Am. J. Physiol.-Regul., Integr. Comp. Physiol. 295 (5), R1631–R1639.

Coyle, S.D., Durborow, R.M., Tidwell, J.H., et al., 2004. Anesthetics in Aquaculture, Vol. 3900. Southern Regional Aquaculture Center Stoneville.

Dubey, H., Kumaresan, R., Mankodiya, K., 2018. Harmonic sum-based method for heart rate estimation using PPG signals affected with motion artifacts. J. Ambient Intell. Humaniz. Comput. 9 (1), 137–150.

Farrell, A.P., Richards, J.G., 2009. Defining hypoxia: an integrative synthesis of the responses of fish to hypoxia. In: Fish Physiology, Vol. 27. Elsevier, pp. 487–503.

FDIR, 2023. Biomassestatistikk etter fylke. URL: https://www.fiskeridir.no/Akvakultur/Tall-og-analyse/Biomassestatistikk/Biomassestatistikk-etter-fylke, Accessed: 09.02.2023.

FOR-2015-06-18-761, 2015. Forskrift om bruk av dyr I Forsøk. URL: https://lovdata.no/dokument/SF/forskrift/2015-06-18-761.

Føre, M., Alfredsen, J.A., Gronningsater, A., 2011. Development of two telemetry-based systems for monitoring the feeding behaviour of Atlantic salmon (Salmo salar L.) in aquaculture sea-cages. Comput. Electron. Agric. 76 (2), 240–251.

Føre, M., Frank, K., Dempster, T., Alfredsen, J.A., Høy, E., 2017a. Biomonitoring using tagged sentinel fish and acoustic telemetry in commercial salmon aquaculture: a feasibility study. Aquacult. Eng. 78, 163–172.

Føre, M., Frank, K., Norton, T., Svendsen, E., Alfredsen, J.A., Dempster, T., Eguiraun, H., Watson, W., Stahl, A., Sunde, L.M., et al., 2017b. Precision fish farming: A new framework to improve production in aquaculture. Biosystems Engineering.

Føre, M., Svendsen, E., Økland, F., Gräns, A., Alfredsen, J.A., Finstad, B., Hedger, R.D., Uglem, I., 2021. Heart rate and swimming activity as indicators of post-surgical recovery time of Atlantic salmon (Salmo salar). Animal Biotelemetry 9 (1), 1–13.

Ghasemi, A., Zahediasl, S., 2012. Normality tests for statistical analysis: a guide for non-statisticians. Int. J. Endocrinol. Metabol. 10 (2), 486.

Golyandina, N., Korobeynikov, A., Zhigljavsky, A., 2018. Singular Spectrum Analysis with R. Springer.

Hanyu, S., Xiaohui, C., 2017. Motion artifact detection and reduction in PPG signals based on statistics analysis. In: 2017 29th Chinese Control and Decision Conference (CCDC). IEEE, pp. 3114–3119.

Hassan, W., Føre, M., Urke, H.A., Kristensen, T., Ulvund, J.B., Alfredsen, J.A., 2019. System for real-time positioning and monitoring of fish in commercial marine farms based on acoustic telemetry and internet of fish (IoF). In: The 29th International Ocean and Polar Engineering Conference. ISOPE.

Haykin, S., 2013. Adaptive Filter Theory (5th Edition). Pearson Education India.

Jónsdóttir, K.E., Hvas, M., Alfredsen, J.A., Føre, M., Alver, M.O., Bjelland, H.V., Oppedal, F., 2019. Fish welfare based classification method of ocean current speeds at aquaculture sites. Aquac. Environ. Interact. 11, 249–261.

Kyriacou, P.A., Allen, J., 2021. Photoplethysmography: Technology, Signal Analysis and Applications. Academic Press.

Lim, P.K., Ng, S.-C., Lovell, N.H., Yu, Y.P., Tan, M.P., McCombie, D., Lim, E., Redmond, S.J., 2018. Adaptive template matching of photoplethysmogram pulses to detect motion artefact. Physiol. Meas. 39 (10), 105005.

Lucas, M., 1994. Heart rate as an indicator of metabolic rate and activity in adult Atlantic salmon, Salmo salar. J. Fish Biol. 44 (5), 889–903.

Madan, A., 2017. Correlation between the levels of SpO2and PaO2. Lung India 34 (3).

Mannheimer, P.D., 2007. The light–tissue interaction of pulse oximetry. Anesth. Analg. 105 (6), S10–S17.

Nitzan, M., Taitelbaum, H., 2008. The measurement of oxygen saturation in arterial and venous blood. IEEE Instrum. Meas. Mag. 11 (3), 9–15.

Oppedal, F., Dempster, T., Stien, L.H., 2011. Environmental drivers of Atlantic salmon behaviour in sea-cages: A review. Aquaculture 311 (1), 1–18.

Park, J., Seok, H.S., Kim, S.-S., Shin, H., 2022. Photoplethysmogram analysis and applications: An integrative review. Front. Physiol. 2511.

Perry, S., Jonz, M., Gilmour, K., 2009. Oxygen sensing and the hypoxic ventilatory response. In: Fish Physiology, Vol. 27. Elsevier, pp. 193–253.

Prahl, S., 1998. Tabulated molar extinction coefficients for hemoglobin in water. Available at https://omlc.org/spectra/hemoglobin/summary.html (Accessed 08.11.2021).

Rankawat, S.A., Rankawat, M., Dubey, R., 2015. ECG artifacts detection in noncardiovascular signals using Slope Sum Function and Teager Kaiser Energy. In: 2015 International Conference on BioSignal Analysis, Processing and Systems (ICBAPS). IEEE, pp. 6–10.

Remen, M., Oppedal, F., Imsland, A.K., Olsen, R.E., Torgersen, T., 2013. Hypoxia tolerance thresholds for post-smolt Atlantic salmon: Dependency of temperature and hypoxia acclimation. Aquaculture 416–417, 41–47.

Remen, M., Sievers, M., Torgersen, T., Oppedal, F., 2016. The oxygen threshold for maximal feed intake of Atlantic salmon post-smolts is highly temperature-dependent. Aquaculture 464, 582–592.

Shin, H., Sun, S., Lee, J., Kim, H.C., 2021. Complementary photoplethysmogram synthesis from electrocardiogram using generative adversarial network. IEEE Access 9, 70639–70649.

Sommerset, I., Walde, C., Bang Jensen, B., Wiik-Nielsen, J., Bornø, B., Oliveira, V., Brun, E., 2023. Fiskehelserapporten 2022, Veterinærinstituttets rapportserie nr 5a/2023. URL: https://www.vetinst.no/rapporter-og-publikasjoner/rapporter/2023/fiskehelserapporten-2022, Accessed: 08.02.2023.

Steinhausen, M., Sandblom, E., Eliason, E., Verhille, C., Farrell, A., 2008. The effect of acute temperature increases on the cardiorespiratory performance of resting and swimming sockeye salmon (Oncorhynchus nerka). J. Exp. Biol. 211 (24), 3915–3926.

Sukor, J.A., Redmond, S., Lovell, N., 2011. Signal quality measures for pulse oximetry through waveform morphology analysis. Physiol. Meas. 32 (3), 369.

Svendsen, E., Føre, M., Økland, F., Gräns, A., Hedger, R.D., Alfredsen, J.A., Uglem, I., Rosten, C., Frank, K., Erikson, U., et al., 2021a. Heart rate and swimming activity as stress indicators for Atlantic salmon (Salmo salar). Aquaculture 531, 735804.

Svendsen, E., Føre, M., Randeberg, L.L., Alfredsen, J.A., 2021b. Design of a novel biosensor implant for farmed Atlantic salmon (Salmo salar). IEEE Sens..

Svendsen, E., Økland, F., Føre, M., Randeberg, L.L., Finstad, B., Olsen, R.E., Alfredsen, J.A., 2021c. Optical measurement of tissue perfusion changes as an alternative to electrocardiography for heart rate monitoring in Atlantic salmon (Salmo salar). Animal Biotelemetry 9 (1), 1–12.

Svendsen, E., Randeberg, L.L., Føre, M., Finstad, B., Olsen, R.E., Bloecher, N., Alfredsen, J.A., 2023. Characterization of optical properties of atlantic salmon (*Salmo salar*) blood. J. Biophotonics Submitted for review.

Thorstad, E.B., Rikardsen, A.H., Alp, A., Økland, F., 2013. The use of electronic tags in fish research–an overview of fish telemetry methods. Turk. J. Fish. Aquat. Sci. 13 (5), 881–896.

Tota, B., Amelio, D., Pellegrino, D., Ip, Y., Cerra, M., 2005. NO modulation of myocardial performance in fish hearts. Comp. Biochem. Physiol. A 142 (2), 164–177.

van der Bijl, K., Elgendi, M., Menon, C., 2022. Automatic ECG quality assessment techniques: A systematic review. Diagnostics 12 (11), 2578.

Vikeså, V., Nankervis, L., Hevrøy, E.M., 2017. Appetite, metabolism and growth regulation in atlantic salmon (Salmo salar L.) exposed to hypoxia at elevated seawater temperature. Aquacult. Res. 48 (8), 4086–4101.

Wypych, G., 2013. Photophysics. In: Handbook of Material Weathering. Elsevier, pp. 1–25. http://dx.doi.org/10.1016/b978-1-895198-62-1.50004-4.

Xiong, J., Cai, L., Jiang, D., Song, H., He, X., 2016. Spectral matrix decomposition-based motion artifacts removal in multi-channel PPG sensor signals. IEEE Access 4, 3076–3086.

Yoshida, M., Hirano, R., Shima, T., 2009. Photocardiography: a novel method for monitoring cardiac activity in fish. Zool. Sci. 26 (5), 356–361.

Zhang, Z., Pi, Z., Liu, B., 2014. TROIKA: A general framework for heart rate monitoring using wrist-type photoplethysmographic signals during intensive physical exercise. IEEE Trans. Biomed. Eng. 62 (2), 522–531.